GeoConvention
Calgary • Canada • March 7-11 2016
OPTIMIZING RESOURCES

Frequency-ray Parameter Domain Full-waveform Inversion

Wenyong Pan and Kris Innanen
CREWES Project, Department of Geoscience, University of Calgary

Summary

Full-waveform inversion (FWI) promises high-resolution estimates of the subsurface model properties. Its computational cost remains an obstacle in practical applications, and research is active in developing efficient FWI implementations. We describe an efficient frequency-ray parameter (f-p) domain FWI equipped with linear phase-encoding in this paper. A slant update strategy with varied ray parameters is proposed to further reduce the computation burden. The proposed strategies can reduce the computation burden significantly but also unfortunately introduce strong cross-talk artifacts. We demonstrate that a partial overlap-frequency strategy is important to suppress these cross-talk artifacts. The frequency-ray parameter domain FWI is implemented with different optimization methods. The f-p domain FWI is then enacted on a Marmousi-II model to demonstrate the effectiveness and efficiency of the combined strategies on reconstructing the velocity model.

Introduction

Full-waveform inversion (FWI) is becoming increasingly popular for building velocity models in oil and gas exploration (Lailly, 1983; Tarantola, 1984; Virieux and Operto, 2009). It promises high-resolution estimates of the model parameters, but this comes at high computational cost. Aiming at reducing the computational cost for FWI, an efficient frequency-ray parameter (f-p) domain FWI with a slant update strategy is developed in this research.

One popular approach for reducing the computational cost of FWI is to employ the phase-encoding technique, which involves the formation of super-gathers from summation of individual shots. Simulation of simultaneous sources can reduce computational cost significantly but at the expense of introducing cross-talk artifacts. Linear phase-encoding strategy is performed by applying linear phase shifts at the source locations and transforming the shot gathers into plane-wave gathers with different ray parameters. In traditional linear-phase encoding (TLPE) method, the cross-talk artifacts are mitigated by stacking a set of ray parameters at each iteration. Because the number of ray parameter gathers is much smaller than the number of common shot gathers in shot-profile (SP) method, the computational cost can be significantly reduced. In this paper, to reduce the computational cost further, we develop a slant update (SU) strategy with linear-phase encoding, in which the gradient is constructed with single ray parameter but the ray parameter varies sequentially or randomly at each iteration.

The gradient-based methods suffer from slow local convergence rate. The Newton-type methods provide quadratic convergence rate but are extremely expensive (Pratt et al., 1998; Pan et al., 2014b, 2015b). The Hessian-free optimization methods employ second-order adjoint-state formulas to compute the Hessian-vector products instead of calculating the Hessian explicitly (Nash, 1985; Pan et al., 2016). In this research, a preconditioned Hessian-free Gauss-Newton (PHFGN) method is also implemented by constructing the gradient and Hessian with the linear phase-encoding. The limited-memory BFGS (*l*-BFGS) method stores the changes of the gradient and model from a limited number of previous iterations and uses the stored information to implicitly form an inverse of the approximated Hessian.

Forward modelling in the f-p domain

The linear phase-encoding is performed by applying linear phase shifts (or time delays in the time domain) at densely distributed sources. A common-receiver gather can be transformed into ray parameter super-gather from a line source wavefield, which is known as $\tau - p$ transform:

$$\tilde{\mathbf{u}}(\mathbf{x}_r, p, \omega) = \sum_{\mathbf{x}_s} \mathbf{u}(\mathbf{x}_r, \mathbf{x}_s, \omega) \exp(i\omega p(\mathbf{x}_s - \mathbf{x}_s^0)), \tag{1}$$

where $\mathbf{x}_r$ and $\mathbf{x}_s$ indicate the locations of receivers and sources. $\mathbf{x}_s^0$ is the location of the initial source. The synthetic ray parameter gather in frequency domain is generated with a line source by applying phase shifts at the source locations. Thus, the corresponding wave equation is given as:

$$\mathbf{L}(\mathbf{x}, \omega)\tilde{\mathbf{u}}(\mathbf{x}, p, \omega) = -\sum_{\mathbf{x}_s} f_s(\omega)\delta(\mathbf{x} - \mathbf{x}_s)\exp(i\omega p(\mathbf{x}_s - \hat{\mathbf{x}}_s)), \tag{2}$$

The solution of equation (2) with a line source can be written as:

$$\tilde{\mathbf{u}}(\mathbf{x}, p, \omega) = \sum_{\mathbf{x}_s} f_s(\omega) G(\mathbf{x}, \mathbf{x}_s, \omega)\exp(i\omega p(\mathbf{x}_s - \hat{\mathbf{x}}_s)). \tag{3}$$

In this research, the linear equations are solved with a direct solver based on multi-frontal Lower Upper (LU) decomposition, which is efficient for a multi-source problem with forward and backward substitutions.

Slant update strategy with linear phase-encoding

The simultaneous source method was first proposed in pre-stack depth migration for addressing the obstacle of high computational cost. The linear phase-encoding strategy is performed by decomposing the densely seismic data into plane-wave domain and choosing a set of ray parameters for modelling, migration and inversion. With the adjoint-state method, the gradient can be constructed by cross-correlating the forward modelled wavefield and backpropagated data residual wavefield (Pratt et al., 1998; Pan et al., 2015a, 2015b):

$$\tilde{\mathbf{g}}(\mathbf{x}, p) = \sum_{\omega} \sum_{\mathbf{x}_s} \sum_{\mathbf{x}_r} \sum_{\mathbf{x}_s'} \Re(\omega^2 f_s(\omega) G(\mathbf{x}, \mathbf{x}_s, \omega) G(\mathbf{x}, \mathbf{x}_r, \omega) \Delta\mathbf{d}^*(\mathbf{x}_r, \mathbf{x}_s', \omega) A^2(\omega) \exp(i\omega p(\mathbf{x}_s - \mathbf{x}_s'))), \tag{4}$$

In traditional linear-phase encoding strategy, the gradient is constructed by stacking sufficient ray parameters from mitigating the cross-talk artifacts:

$$\tilde{\mathbf{g}}(\mathbf{x}) = \sum_{\mathbf{p}} \sum_{\omega} \sum_{\mathbf{x}_s} \sum_{\mathbf{x}_r} \sum_{\mathbf{x}_s'} \Re(\omega^2 f_s(\omega) G(\mathbf{x}, \mathbf{x}_s, \omega) G(\mathbf{x}, \mathbf{x}_r, \omega) \Delta\mathbf{d}^*(\mathbf{x}_r, \mathbf{x}_s', \omega) A^2(\omega) \exp(i\omega \mathbf{p}(\mathbf{x}_s - \mathbf{x}_s'))), \tag{5}$$

In shot-profile (SP) method, number of $2 \times N_s \times N_f$ forward modelling problems are required for gradient calculation, which is proportional to the number of sources N_s. Because the number of ray parameters N_p is far smaller than the number of sources, the computational burden at each iteration in TLPE method is greatly reduced. In this research, for reducing the computational burden further, we develop a slant update (SU) strategy, in which the slant gradient with single ray parameter (equation (4)) is used to update the model instead of the phase-encoded gradient with stacking ray parameters (equation (5)). Thus, number of N_f forward modelling problems are required for gradient construction at each non-linear iteration.

Examples

The Marmousi-II model has 244 X 681 grid cells with a grid interval of 10 m in both horizontal and vertical directions. Figures 1a and 1b show the true Marmousi-II P-wave velocity model and initial P-wave velocity model respectively. The initial velocity model is obtained by smoothing the true model with a Gaussian function.

We perform two different frequency selection strategies for comparison with *l*-BFGS optimization method, which are mono-frequeny and partial overlap-frequency strategies. For the SU strategy, we compare two

different ray parameter selections. The random SU is implemented by randomly selecting the ray parameter in the range of [-0.05 s/km, 0.05 s/km] at each iteration. While for the sequential SU, the ray parameter is sequentially changed from -0.05 s/km to 0.05 s/km.

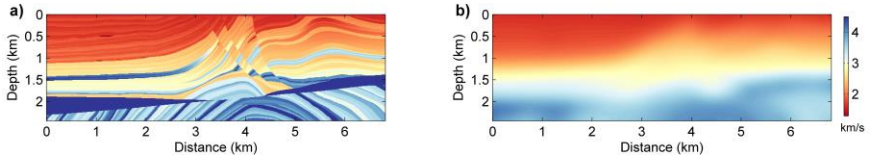

Figure 1. (a) True P-wave velocity model; (b) Initial P-wave velocity model.

We obtain the inversion results by slant update strategy with fixed ray parameters p=-0.01 s/km and p=-0.03 s/km, as shown in Figures 2a and 2b respectively. The inversion results with one fixed ray parameters for all iterations are contaminated by artifacts seriously and the main geological structures of the model are obscure. Figures 2c and 2e show the inversion results by random and sequential SU with mono-frequency strategy. Even though, the inversion results become much better, they are still contaminated by strong cross-talk artifacts. We next carry out the partial overlap-frequency strategy for inversion. Figures 2d and 2f show the inversion results by random and sequential SU with partial overlap-frequency strategy. Compared to Figures 2c and 2e, it can be observed that the artifacts have been suppressed effectively and the inversion results have been improved significantly, which demonstrate the importance of inverting multiple frequencies simultaneously for slant update strategy.

Figures 3a and 3c show the inverted velocity models by mono-frequency TLPE method with Np=7 and Np=11 respectively. As we can see, compared to Figures 2c and 2e, the inversion results have been improved obviously by stacking ray parameters at each iteration with mono-frequency strategy. Figures 3b, 3d and 3f are the inverted models using TLPH (Np=7), TLPH (Np=11) and SP methods with partial overlap-frequency strategy, which are better than those obtained with mono-frequency strategy. We also note that with partial overlap-frequency strategy, SU methods can get inversion results comparable to those by TLPE and SP methods.

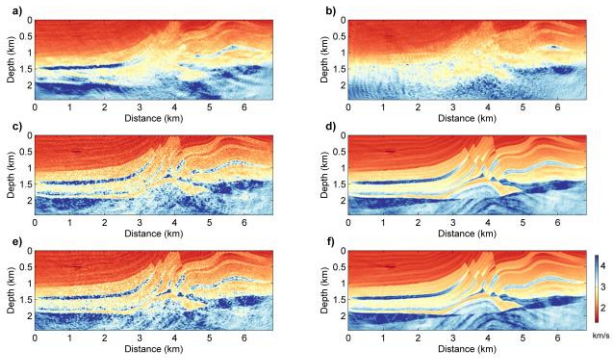

Figure 2. (a) Mono-frequency slant update with p=-0.01 s/km; (b) Mono-frequency slant update with p=-0.03 s/km; (c) Mono-frequency random slant update; (d) Partial overlap-frequency random slant update; (e) Mono-frequency sequential slant update; (f) Partial overlap-frequency sequential slant update.

Figure 4 show the RLSE vs. Number of forward modelling problems solved for different encoding methods with partial overlap-frequency strategy. Figure 4b gives the enlarged view of Figure 4a. It is observed that to obtain comparable quality inversion results, sequential SU strategy reconstructs the velocity model most efficiently compared to TLPE and SP methods. It is verified that the proposed strategies can reconstruct the velocity model well with reducing the computational burden considerably.

We also obtain the inversion results in f-p domain with different optimization methods including SD, NCG, and preconditioned Hessian-free Gauss-Newton methods, as shown in Figures 5a, 5b, and 5c. Figures 6a and 6b show the convergence rate and RLSE vs. Number of forward modelling problems solved by

different optimization methods. As we see, the PHFGN method gives fastest convergence rate while *l*-BFGS can reconstruct the velocity model most efficiently.

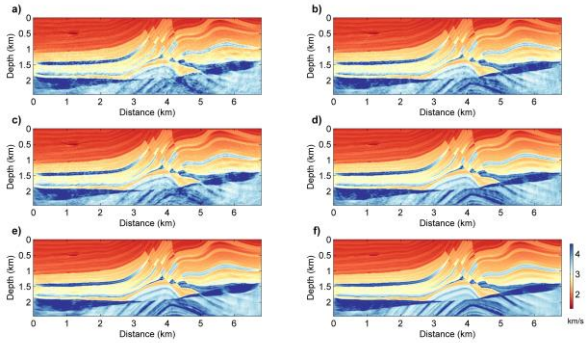

Figure 3. (a) Mono-frequency TLPE with Np=7; (b) Partial overlap-frequency TLPE with Np=7; (c) Mono-frequency TLPE with Np=11; (d) Partial overlap-frequency TLPE with Np=11; (e) Mono-frequency SP; (f) Partial overlap-frequency SP.

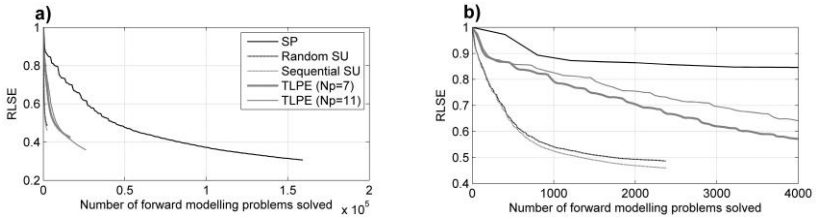

Figure 4. RLSE vs. Number of forward modelling problems solved. (b) is enlarged view of (a).

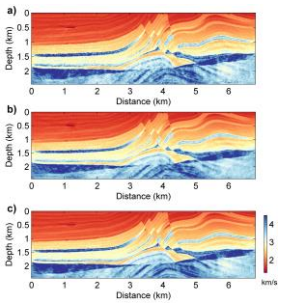

Figure 5. Inversion results by SD, NCG and PHFGN methods

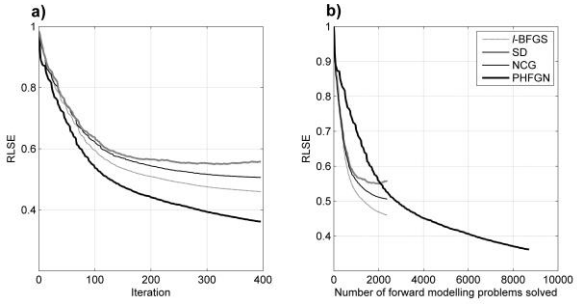

Figure 6. Convergence rate (a) and RLSE vs. Number of forward modelling problems solved (b).

Conclusions

In this paper, employing a linear phase-encoding technique, we develop an efficient frequency-ray parameter (f-p) domain FWI with slant update strategy for reducing the computational burden. The gradient constructed with single ray parameter is used to update the model at each iteration but the ray parameter varies as iteration proceeds. The numerical examples are illustrated to show that the slant update strategy can obtain comparable quality inversion results with reducing the computational burden significantly in comparison with traditional methods. We also illustrate with numerical examples that a preconditioned Hessian-free Gauss-Newton method provides fastest convergence rate while the *l*-BFGS method can reconstruct the velocity model most efficiently.

Acknowledgements

This research was supported by the Consortium for Research in Elastic Wave Exploration Seismology (CREWES) and National Science and Engineering Research Council of Canada (NSERC, CRDPJ 379744-08).

References

Lailly, P., 1983, The seismic inverse problem as a sequence of before stack migration: Conference on Inverse Scattering, Theory and Applications, SIAM, Expanded Abstracts, 206-220.

Nash, S. G., 1985, Preconditioning of truncated-newton methods: SIAM J. Sci. Statist. Comput, 6, 599-616.

Pratt, R. G., C. Shin, and G. J. Hicks, 1998, Gauss-Newton and full Newton methods in frequency-space seismic waveform inversion: Geophysical Journal International, **133**, 341-362.

Pan, W., K. A. Innanen, and G. F. Margrave, 2014a, A comparison of different scaling methods for least-squares migration/inversion: EAGE Expanded Abstracts, We G103 14.

Pan, W., K. A. Innanen, G. F. Margrave, and D. Cao, 2015a, Efficient pseudo-Gauss-Newton full-waveform inversion in the $\tau - p$ domain: Geophysics, **80**, no. 5, R225-R14.

Pan, W., K. A. Innanen, G. F. Margrave, M. C. Fehler, X. Fang, and J. Li, 2015b, Estimation of elastic constants in HTI media using Gauss-Newton and Full-Newton multi-parameter full waveform inversion: SEG Technical Program Expanded Abstracts, 1177-1182.

Pan, W., G. F. Margrave, and K. A. Innanen, 2014b, Iterative modeling migration and inversion (IMMI): Combining full waveform inversion with standard inversion methodology: SEG Technical Program Expanded Abstracts, 938-943.

Pan, W., K. A. Innanen, and W. Liao, 2016a, Accelerating the Hessian-free Gauss-Newton Full-waveform Inversion via Preconditioned Conjugate Gradient Method: GeoConvention, 2016.

Tarantola, A., 1984, Inversion of seismic reflection data in the acoustic approximation: Geophysics, **49**, 1259-1266.

Virieux, A. and S. Operto, 2009, An overview of full-waveform inversion in exploration geophysics: Geophysics, **74**, no. 6, WCC1-WCC26.